IEEE Access
Multidisciplinary | Rapid Review | Open Access Journal

Received 9 November 2023, accepted 17 November 2023, date of publication 25 December 2023, date of current version 2 April 2024.

Digital Object Identifier 10.1109/ACCESS.2023.3346674

RESEARCH ARTICLE

Optimal Fuzzy Logic Enabled EEG Motor Imagery Classification for Brain Computer Interface

EUNMOK YANG[1], K. SHANKAR[2], (Senior Member, IEEE), ESWARAN PERUMAL[3], AND CHANGHO SEO[4]

[1]Department of Financial Information Security, Kookmin University, Seoul 02707, Republic of Korea
[2]Department of Computer Science and Engineering, Saveetha School of Engineering, Saveetha Institute of Medical and Technical Sciences, Chennai 602105, India
[3]Department of Computer Applications, Alagappa University, Karaikudi 630003, India
[4]Department of Convergence Science, Kongju National University, Gongju, Chungcheongnam 32588, South Korea

Corresponding author: Changho Seo (chseo@kongju.ac.kr)

This work was supported in part by the Institute of Information and Communications Technology Planning and Evaluation (IITP) funded by the Korean Government through MSIT (Development of User Identity Certification and Management Technology for Self-Sovereign Identity Applications) under Grant 2021-0-00565 and in part by the Research Grant from Kongju National University in 2024.

ABSTRACT Brain-computer interface BCI) is a technology that assists in straight link among the human brain as well as external devices like computers or robotic systems, without including muscles and peripheral nerves. BCI allows individuals with motor disabilities to manage external devices with the aid of brain signals such as motor imagery detected from electroencephalography (EEG) signals. An EEG Motor Imagery Classification for BCI is a specific application of EEG in which brain signals directly related to motor imagery tasks are analyzed and classified to control external devices or applications, namely robotic systems or computers. In this regard, the study introduces a Jellyfish Optimization with Fuzzy Logic Enabled EEG Motor Imagery Classification for Brain Computer Interface (JFOFL-MICBCI) technique. The JFOFL-MICBCI technique aims to exploit the fuzzy logic system with metaheuristics for classifying EEC motor imagery signals. It initially executes Continuous Wavelet Transform (CWT) for transforming 1D-EEG signals into 2D time-frequency amplitude ones. For feature extraction, the JFOFL-MICBCI technique uses the SqueezeNet method, and its hyperparameters can be adjusted by the employ of the JFO system. The JFOFL-MICBCI method exploits the adaptive neuro-fuzzy inference system (ANFIS) approach for performing the classification process. A comprehensive range of experiments has been accompanied to demonstrate the higher efficiency of the JFOFL-MICBCI technique. The obtained results inferred the better of the JFOFL-MICBCI technique with other recent systems.

INDEX TERMS EEG signals, human–computer interaction, fuzzy logic, brain–computer interface, meta-heuristics.

I. INTRODUCTION

A Brain-Computer Interface (BCI) is an evolving technique which is mainly designed to measure and transform brain activity into artificial outputs, which can include improving, restoring, replacing, supplementing, or enhancing normal central nervous system outputs [1], [2], [3]. Motor Imagery (MI) is a powerful skill wherein the user mentally envisions motor movements without actual physical execution, involving no activation of peripheral nerves or muscles. A Motor Imagery Brain-Computer Interface (MI-BCI) works as a method to transform brain signals produced in these imaginings into activity order [4]. MI-BCI technique chiefly uses electroencephalogram (EEG) to measure brain movement [5]. EEG offers higher temporal resolution, could be moveable at a comparatively lower price, and characterizes synchronous electrical signals generated by the brain [6]. However, recorded EEG signals have been nonstationary and endure a reduced spatial resolution as well as a lower signal-to-noise ratio (SNR) [7], [8], [9]. Thus, using them in the BCI technique can be required to employ innovative signal processing models for cleaning the information in artefacts and extracting related frequency, temporal, and spatial data in the signals for classification issues [10].

The associate editor coordinating the review of this manuscript and approving it for publication was Giacinto Barresi.

Conventionally, MI-BCIs work on machine learning (ML) approaches so that spatial features related to action imaginings can be identified [11], [12]. The imagining of both right and left body movements is combined with lateralized event-related (de)synchronization (ERS or ERD) from beta (13 to 30 Hz) and mu (7 to 13 Hz) frequency bands of EEG signals [13]. These brain action features are generally collected using the Common Spatial Pattern (CSP) technique and serve as input to the ML approach categorizing imagined body actions [2], [14], [15]. As a result, the method depends on the user for deliberately modulating its brain activity, thereby, the lateralization is identified [16], [17]. With the fast growth of high-power computing devices, deep learning (DL) has become extremely popular in several domains [18], [19]. A great benefit of bringing DL technology into the BCI technique is that feature extraction and classification stages have been learned directly from information, also referred to as 'end-to-end' learning [20].

This article presents a Jellyfish Optimization with Fuzzy Logic Enabled EEG Motor Imagery Classification for Brain Computer Interface (JFOFL-MICBCI) technique. A purpose of the JFOFL-MICBCI methodology is to feat the FL system with metaheuristics for the classification of EEC motor imagery signals. It initially executes Continuous Wavelet Transform (CWT) for transforming 1D-EEG signals into 2D time-frequency amplitude ones. For feature extraction, the JFOFL-MICBCI method uses the SqueezeNet technique, and its hyperparameters can be adjusted by utilizing the JFO system. The JFOFL-MICBCI method exploits the adaptive neuro-fuzzy inference system (ANFIS) approach to execute the classification process. A comprehensive range of experiments has been accompanied to establish a high solution of the JFOFL-MICBCI process.

II. RELATED WORKS

EEG motor imagery classification is a pivotal component in the field of BCI research. The ability to decode and interpret neural signals related to motor imagery tasks holds tremendous promise in empowering individuals with neurodegenerative disorders or severe physical impairments to interact with and control external devices through the power of their thoughts. This section offers an extensive exploration of the existing EEG motor imagery classification models in the BCI domain. By examining the existing studies, methodological advancements, and the challenges faced by researchers, a thorough understanding of the current state of the art can be made and identify critical avenues for further exploration and improvement in this exciting and transformative field.

Sharma et al. [21] offer a widespread comparison among classification approaches and suggest the importance of DL-based BCI methods, particularly multi-layer perceptron (MLP). Briefly, with EEG signal during motor imagery task, SVM demonstrates the short training time and prediction speed with similar performance amongst classical ML-based algorithms. Subasi et al. [22] introduced an automatic detection of MI tasks. Wavelet Packet Decomposition (WPD), efficient hybridization of the Multiscale Principal Component Analysis (MSPCA), ensemble learning-based classifiers, and statistical features extraction from subbands for classification of MI task. The EEG signal is denoised and segmented and is accomplished with Daubechies model-based wavelet transform (WT). Liu et al. [23] introduce a Matlab-based real-time MI-BCI (MartMi-BCI) software that includes a model training platform (MTP) and a real-world EEG analysis platform (RTEEGAP).

In [24], authors proposed a novel method that depends on the 10-layer one-dimensional convolutional neural networks (1D-CNNs) to categorize 5 brain states (a 'baseline' class and four MI classes) employing a data augmentation method and a small amount of EEG channels. Moreover, a transfer learning (TL) model was employed to remove crucial attributes from EEG group datasets. Mirzaei and Ghasemi [25] introduced a new feature extraction technique that results in the potential performance of MI classification. The time series of the EEG channel was divided into temporal blocks and calculate connectivity matrix for all the blocks utilizing adaptive sparse representation (ASR). A vibrant connectivity pattern is constructed using 3D tensors. Next, nonlinear convolutional autoencoders (CAE) or kernel PCA is exploited to this tensor for learning discriminative representation. The author in [26], intends to help communities affected by this disorder with the improvement of a technique that can detect the objective to perform the movement in the upper limits of the body. Furthermore, a digital signal filter was intended to keep the frequency band.

Kamble et al. [27] exploited new adaptive signal decomposition techniques, namely variational nonlinear chirp mode decomposition, empirical WTs, variational mode decomposition, and empirical mode decomposition for decomposing EEG signals into different modes. Dhiman [28] applied the Pearson correlation coefficient (PCC) method for selecting channels for signals of EEG. WPD is exploited for extracting features. The channel selection method and WPD are incorporated for categorizing MI signals. Lastly, feature extraction was categorized using support vector machines (SVMs) and K-nearest neighbour (KNN).

Sadiq et al. [29] developed a simple and robust mechanical multivariate empirical wavelet transform (MEWT) model for decoding dissimilar MI challenges. In [30], a new design is presented for the automatic precise detection of MI tasks. Primary, raw EEG signals denoised by multiscale main factor study. Then, denoised signals decayed by experiential WT in various manners. In 3rd stage, dual-dimensional modelling of types is proposed to recognize differences in diverse signals. In [31], a new and effective computer-aided diagnosis architecture is presented for the detection of MI-EEG signals. Foremost, a multivariate variation mode decomposition (MVMD) technique is used to get combined modes in occurrence scale through entire networks.

Geng et al. [32] present a processing algorithm for EEG signals with the combination of independent component analysis (ICA), WT and common spatial pattern (CSP). Firstly, the ICA model is used to break the EEG signals into independent components. Next, these components are decomposed by WT to attain the wavelet coefficient of all the independent sources. Sun et al. [33] introduced an end-to-end DL architecture named EEG channel active inference neural network (EEG-ARNN), which is based on a graph convolutional neural network (GCN) to utilize the correlation of signals in the spatial and temporal domains. Tiwari [34] established a Logistic S-shaped Binary Jaya Optimization Algorithm (LS-BJOA), which integrates a logistic mapping with the Jaya optimization algorithm (IOA) to mitigate the computation burden made by the channel.

III. THE PROPOSED MODEL

This work presents an automated EEG Motor Imagery Classification for BCI using the JFOFL-MICBCI method. The main goal of the JFOFL-MICBCI technique is to utilize the FL system with metaheuristics for the classification of EEC motor imagery signals. It comprises different subprocesses such as CWT-based pre-processing, SqueezeNet feature extractor, JFO-based hyperparameter tuning as well and ANFIS-based classification. Fig. 1 depicts the entire flow of the JFOFL-MICBCI algorithm.

A. PRE-PROCESSING

Firstly, the data preprocessing takes place in two major phases namely MSPCA-based denoising and CWT-based decomposition. MSPCA is a robust mechanism widely known for decreasing noise in EEG signals. This technique excels at improving the quality of EEG information by effectively eliminating noise while preserving important neural data. By carrying out a multiscale analysis, MSPCA can tackle noise components at different temporal and spatial scales, making it suitable for the varied nature of EEG signals. By using PCA, it reaches dimensionality reduction, efficiently separating noise from the neural signal components. MSPCA is especially valuable in cases where sources of noise are statistically independent of the EEG signals, as it extracts independent components. Furthermore, its adaptability allows for fine-tuning to suit the certain requirements of the EEG information and the task at hand. The wide-ranging use of MSPCA in EEG signal processing and its established efficiency make it a reliable choice for denoising, contributing to the enhancement of the data quality before succeeding processing steps namely classification and feature extraction.

For decomposition, CWT is a popularly adopted strategy to convert a 1D signal to a 2D matrix in the frequency domain [35]. When compared to the conventional cosine and Fourier transform (FT), WT is an efficient technique as a time-frequency transform. As compared with FT, which generates a spectrogram with fixed time-frequency resolution, WT integrates different scales, and for such reasons, it provides optimum time-frequency resolution. The wavelet filtering bank exploits the analytic Morse wavelet with the time-bandwidth product and symmetry parameters equivalent to 60 and 3, correspondingly. According to the energy extent of the wavelet from the time-frequency domain, the wavelet maximum and minimum scales can automatically be defined. Meanwhile, the scalogram image of WT is 69×400, rescaled to 224×224 via bicubic interpolation. This step is essential since pre-trained GoogLeNet takes input with the dimension of 224×224.

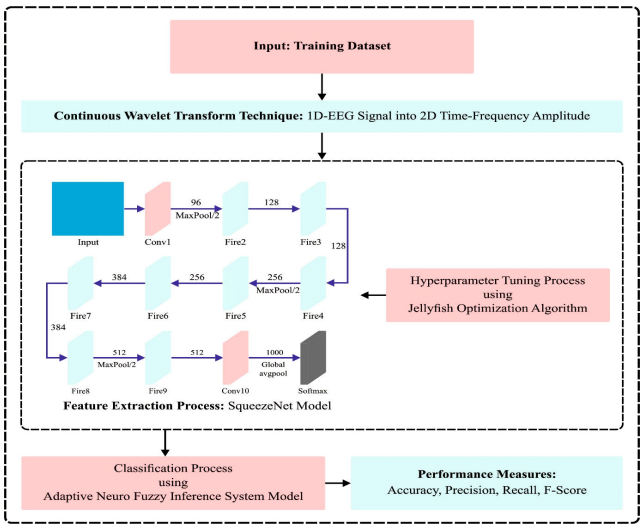

FIGURE 1. The overall flow of the JFOFL-MICBCI algorithm.

B. OPTIMAL SqueezeNet-BASED FEATURE EXTRACTION

To derive features effectually, the SqueezeNet model is used. Classical structures have the demerits of demanding an enormous number of parameters for training. So, researcher workers introduced ''SqueezeNet'' a new framework that has a very small method size and needs some training parameters [36]. The architecture of SqueezeNet comprises 8 fire modules and one convolutional layer. A fire module has a convolution layer with a 1×1 filter as well as an ''n'' filter size, signified as a ''Squeeze'' layer. Next, there exist dual corresponding layers, called as ''Expand'' layer. The primary ''Expand'' layer has 4n filters as well as a 1×1 filter size. Likewise, the 2^{nd} ''Expand'' layer has 4n filters and a 3×3 filter size. The ''Squeeze'' and ''Expand'' layers are in sequence. A max-pooling layer is exploited (stride $= 2$) after 1^{st} convolution layer and 2^{nd} and 4^{th} fire modules reduce the size of feature maps by half. A fully connected (FC) layer (weight $= 1000$) is exploited after the last fire module that transforms feature maps into a one-dimensional vector. While these feature vectors passed over the average pooling layer. Every prior convolution layer follows a rectified linear unit (ReLU) function. At last, the softmax layer adapts feature vectors into double classification.

A JFO algorithm was applied for the hyperparameter selection process. JFO is a recent metaheuristic optimization technique derived from the jellyfish (JF) behaviours for searching for food in the ocean [37]. This technique was

stimulated by the movement patterns and exploration strategy of JF in the ocean. In this work, the quantity of food at dissimilar positions differs; thus, by comparing the food proportion of JF, the optimal position was easily traced. This technique provides an optimum balance between exploitation and exploration strategies, and therefore, the optimum solution can be attained in a shorter period. It is essential to know about the passive and active movements of ocean currents inside the JF swarm to simulate the search behaviour of the JF. This algorithm makes use of three fundamental rules.

1. A ''time control mechanism'' permits JF to shift between going inside the swarm and the ocean current.

2. Food availability in the ocean.

3. The region and its objective functions have a considerable effect that several foods are available.

Ocean current was evaluated using Eq. (1):

$$X_i(t+1) = X_i(t) + rand(0,1) * \left(X'' - \beta * rand(0,1)\right), \tag{1}$$

In Eq. (1), the updated position can be defined by $X_i(t+l)$, the mean location is μ, and β shows the distribution coefficient ($\beta > 0$). In the swarming movement, JFs are active (type B, j) and passive (type A, i). The movement of JF in the positions is represented as type A, and a location change is shown in Eq. (2), where $\gamma > 0$ denotes the motion coefficient. L_b and U_b are the lower and upper bounds for the objective function. Type B motion of the JF (j) in opposition to the type A motion. Eq. (4) is used to update the position, and Eq. (3) is regarded to estimate the direction of motion.

Where and refer to the time control mechanism. Values differ from zero to one and signify the time period at a specific instant.

$$X_i(t+1) = X_i(t) + \gamma * rand(0,1) * (U_B - L_B), \tag{2}$$

$$|Direction| = \begin{cases} Xj(t) - Xi(t); iff\ (Xi) \geq f(Xj), \\ Xi(t) - Xj(t); iff\ (Xi) < f(Xi). \end{cases} \tag{3}$$

where c(t) and c_o refer to the time control mechanism. c(t) values differ from zero to one, and t signifies the time period at a specific instant.

$$X_i(t+1) = X_i(t) + rand(0,1) * Direction, \tag{4}$$

$$c(t) = \left|1 - \frac{t}{\mathrm{Max}_{iteration}}\right| \times (2 * rand(0,1) - 1) \tag{5}$$

Population initialization can be performed by using Eq. (6):

$$X_{i+1} = a * X_i * (1 - x(i)); 0 \leq X_o \leq 1, \tag{6}$$

Here, X_i refers to the logistic chaotic value of i^{th} JF, $X_0 \in (0, 1)$, and the value of ''a'' is selected as 4.0. Eq. (6), denotes the ''initialization stage'', which is an initial step in the JFO technique, and Eq. (5) shows the time control mechanism in JFO. The next step is to set boundary conditions for dissimilar functions. These conditions are significant such that JF doesn't move outside the searching region. Eq. (7) provides a limit of JF in a boundary condition or search region to JF. A JF is positioned in $X_{i,d}$ at *the* d^{th} dimension. $U_{b,d}$, and $L_{b,d}$ denote upper and lower boundaries in search space .

$$\begin{aligned} X'_{i,d} &= X_{i,d} - U_{b,d} + L(d); if\ X_{i,d} > U_{b,d}, \ldots \\ X_{i,d} &= X_{i,d} - L_{b,d} + U(d); if\ X_{i,d} < L_{b,d}. \end{aligned} \tag{7}$$

The JFO method derives a fitness function (FF) to obtain the high efficiency of the classifier. It describes a positive value to characterize the optimal results of the solution candidate. The decline of the classifier error rate is assumed as an FF.

$$\begin{aligned} fitness(x_i) &= ClassifierErrorRate(x_i) \\ &= \frac{No.\ of\ misclassified\ samples}{Total\ No.\ of\ samples} * 100 \end{aligned} \tag{8}$$

C. FUZZY LOGIC-BASED CLASSIFICATION

The ANFIS model is used for the classification process. ANFIS incorporates the benefits of FL systems and neural networks (NNs) [38]. It exploits a learning model of NN for the automatic extraction of input and rules of sampling datasets, thus making an ANFIS that consists of 5 layers. ANFIS is a variant of artificial intelligence (AI) technology that incorporates the power of ANN or FL systems. ANFIS is a hybrid mechanism that exploits FIS embedding in NN architecture. The FIS model of ANFIS employed to represent linguistic procedures that define the relation between input and output in a model. Based on input-output training datasets, the NN model was used to adjust the parameters of the FIS, such as membership function parameters and the rule weights. This allows the ANFIS to predict new input values and ''learn'' the connections between inputs and outputs. Fig. 2 displays the framework of ANFIS. ANFIS is exploited for an enormous amount of work, including function approximation, time series prediction, and control. It is a new type of FL system that is capable of learning and adapting a learning model. Based on the training dataset, the learning mechanism adjusts the parameters of the FL system to improve efficiency. The Adaptive component of ANFIS makes it highly relevant for applications whereby basic procedure is exposed to variations over time, i.e., modelling dynamic systems.

It is an addition to conventional FL systems and has a similar architecture that encompasses FIS, output, and input layers. In summary, ANFIS incorporates the ability to describe uncertain or vague knowledge of FIS with the ability to learn from data of the NN.

Layer 1: Every node is an adaptive node. The output is a fuzzy membership grade of input, as given below:

$$O_i^1 = \mu_{A_i}(x)\ i = 1, 2 \tag{9}$$

$$O_i^1 = \mu_{B_{i-2}}(y)\ i = 3, 4 \tag{10}$$

where $\mu_{A_i}(x), \mu_{B_{i-2}}(y)$ adopted a fuzzy membership function.

Layer2: The node is a fixed node. They were labelled with M and played a simple multiplier, as shown in the following.

$$O_i^2 = \omega_i = \mu_{A_i}(x)\,\mu_{B_i}(y)\ i = 1, 2 \tag{11}$$

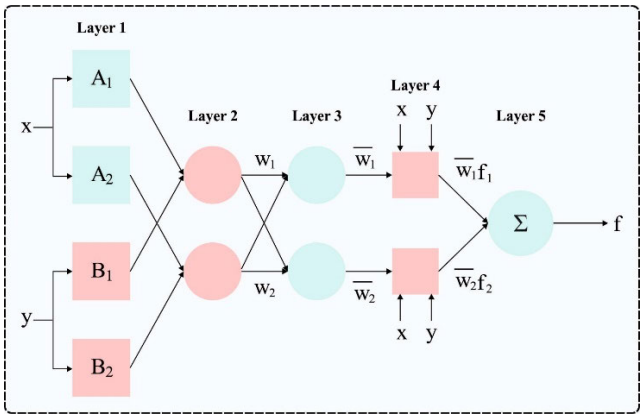

FIGURE 2. ANFIS structure.

Layer3: The node was fixed. They were labelled with N, which represents that they implement normalization to firing strength from the previous layer as follows.

$$O_i^3 = \omega_i = \frac{\omega_i}{\omega_1 + \omega_2} i = 1, 2 \tag{12}$$

Layer4: The node was adaptive. Each output node is a product of the 1st-order Sugeno model (1st-order polynomial), and normalized firing strength, as shown below:

$$O_i^4 = \overline{\omega}_i f_i = \overline{\omega}_i \left(p_i x + q_i y + r_i\right) i = 1, 2 \tag{13}$$

Layer5: There is one fixed node labelled with S. These nodes play as a summation of all the incoming signals.

$$O_i^5 = \sum_{i=1}^{2} \overline{\omega}_i f_i = \frac{\sum_{i=1}^{2} \omega_i f_i}{\omega_1 + \omega_2} \tag{14}$$

The concluding output of ANFIS is shown below.

$$f_{out} = \overline{\omega}_1 f_1 + \overline{\omega}_2 f_2 = \frac{\omega_1}{\omega_1 + \omega_2} f_1 + \frac{\omega_2}{\omega_1 + \omega_2} f_2 \tag{15}$$

IV. RESULTS AND DISCUSSION

The experimental results of the JFOFL-MICBCI approach were tested on 2 databases containing BCI competition 2003 dataset-III and BCI competition-IV database 2b. BCI competition 2003, database-III [39], contains 3-channel EEG data in normal females for the imagination of right and left-hand actions. BCI competition-IV database 2b contains nine subjects, all with five sessions of MI experimentally. Among that, the primary two sessions can be confirmed with no feedback, and the remaining three sessions can be integrated with online feedback [40].

Table 1 and Fig. 3 depict the classifier outcome of the JFOFL-MICBCI model on the BCI Competition-III database. The results imply effectual results of the JFOFL-MICBCI technique under all runs.

For instance, on run1, the JFOFL-MICBCI technique offers $prec_n$ of 98.61%, $reca_l$ of 97.29%, $accu_y$ of 98.01%, and F_{score} of 98.13%, respectively. Also, on run2, the JFOFL-MICBCI system attains $prec_n$ of 98.76%, $reca_l$ of 97.46%, $accu_y$ of 98.05%, and F_{score} of 98.10% correspondingly. Afterwards, on run4, the JFOFL-MICBCI approach obtains $prec_n$ of 94.76%, $reca_l$ of 98.65%, $accu_y$ of 96.77%, and F_{score} of 96.80%, respectively. Eventually, on run5, the JFOFL-MICBCI methodology gains $prec_n$ of 95.98%, $reca_l$ of 97.47%, $accu_y$ of 96.63%, and F_{score} of 96.56% correspondingly.

TABLE 1. Classifier outcome of JFOFL-MICBCI technique on BCI Competition-III database.

BCI Competition-III Database				
No. of iterations	$Prec_n$	$Reca_l$	$Accu_y$	F_{score}
Run 1	98.61	97.29	98.01	98.13
Run 2	98.76	97.46	98.05	98.10
Run 3	98.82	100.29	99.64	99.61
Run 4	94.76	98.65	96.77	96.80
Run 5	95.98	97.47	96.63	96.56
Average	97.39	98.23	97.82	97.84

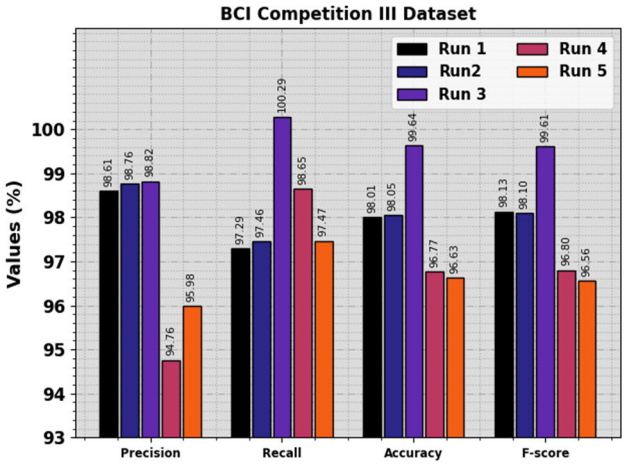

FIGURE 3. Classifier outcome of JFOFL-MICBCI technique on BCI Competition-III database.

Table 2 and Fig. 4, the comparative investigation of the JFOFL-MICBCI approach with present systems on the BCI Competition-III database [41]. The outcomes imply the effectual outcomes of the JFOFL-MICBCI technique exhibit improved outcomes. Based on $accu_y$, JFOFL-MICBCI method offers increasing $accu_y$ of 97.82% while Adaptive PP-Bayesian, STFT-DL, Enhanced GA FKNN-LDA, WTSE-SVM, CWTFB-TL, and AORNDL-MIC approaches obtain decreasing $accu_y$ values of 90%, 90%, 84%, 86.40%, 95.71%, and 96.14% correspondingly.

Fig. 5 illustrates the training accuracy TR_accu_y and VL_accu_y of the JFOFL-MICBCI algorithm on the BCI Competition-III database. TL_accu_y is described by the estimate of the JFOFL-MICBCI procedure on the TR database, whereas VL_accu_y is intended to estimate performance on a distinct testing database. The outcomes exhibit that TR_accu_y and VL_accu_y increase with an upsurge in epochs. Therefore, the performance of the JFOFL-MICBCI model enhances on TR and TS database by a growth in the sum of epochs.

TABLE 2. *Accu$_y$* outcome of JFOFL-MICBCI algorithm with other methods on BCI Competition-III database.

BCI Competition-III Database Methods	Accuracy
Adaptive PP-Bayesian	90.00
STFT-DL	90.00
Optimized GA FKNN-LDA	84.00
WTSE-SVM	86.40
CWTFB-TL	95.71
AORNDL-MIC	96.14
JFOFL-MICBCI	97.82

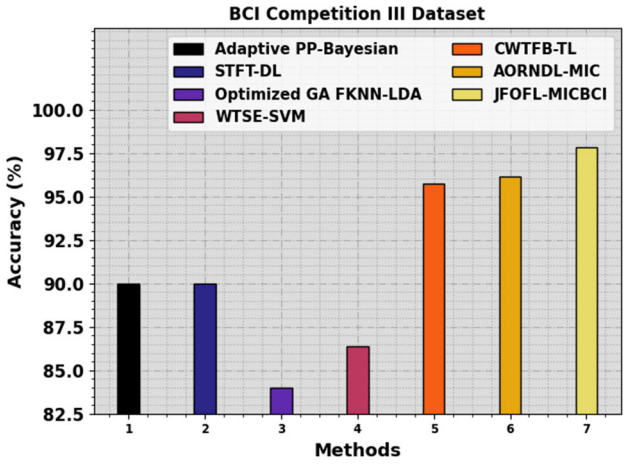

FIGURE 4. *Accu$_y$* outcome of JFOFL-MICBCI system on BCI Competition-III database.

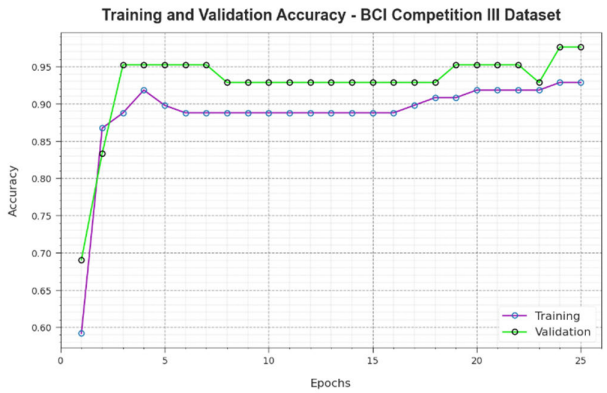

FIGURE 5. *Accu$_y$* curve of JFOFL-MICBCI technique on BCI Competition-III database.

In Fig. 6, *TR_loss* and *VR_loss* analysis of the JFOFL-MICBCI approach on the BCI Competition-III database is exposed. *TR_loss* defines error between predictive solution as well as original values on TR data. *VR_loss* signifies the extent of the outcome of the JFOFL-MICBCI technique on separate validation data. The results direct that *TR_loss* and *VR_loss* incline to reduce with rising epochs. It exposed the greater outcome of the JFOFL-MICBCI system and its capability to make accurate classifications. The smaller value of *TR_loss*, as well as *VR_loss*, establishes a greater outcome of the JFOFL-MICBCI method on capturing patterns and relationships.

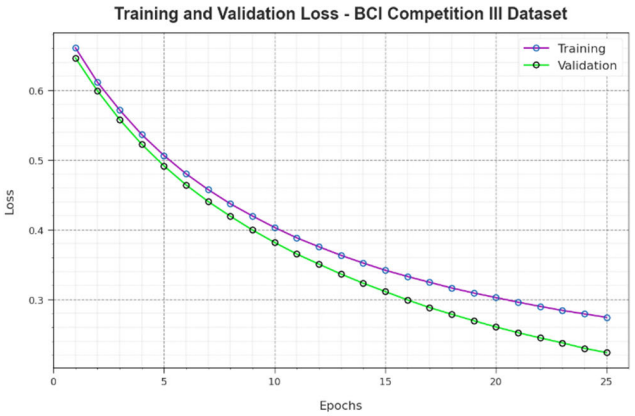

FIGURE 6. Loss curve of JFOFL-MICBCI technique on BCI Competition-III database.

TABLE 3. Training *accu$_y$* outcome of JFOFL-MICBCI technique with distinct runs and samples on BCI Competition-IV database.

BCI Competition-IV Database					
No. of runs	**S1**	**S2**	**S3**	**S4**	**S5**
Run 1	88.62	86.51	89.54	87.72	85.60
Run2	72.68	84.76	81.70	95.65	86.52
Run 3	85.73	97.74	95.52	99.55	89.73
Run 4	83.67	92.51	76.64	90.54	92.51
Run 5	83.65	82.59	87.52	92.80	82.75
Average	**82.87**	**88.82**	**86.18**	**93.25**	**87.42**
No. of runs	**S6**	**S7**	**S8**	**S9**	**Average**
Run 1	77.58	84.50	97.65	84.50	**86.91**
Run2	80.51	92.67	84.78	93.76	**85.89**
Run 3	91.63	86.63	90.59	88.52	**91.74**
Run 4	93.67	82.63	89.58	96.60	**88.71**
Run 5	88.53	96.62	90.69	82.74	**87.54**
Average	**86.38**	**88.61**	**90.66**	**89.22**	**88.16**

Table 3 and Fig. 7 represent an extensive classification result of the JFOFL-MICBCI technique on the BCI Competition-IV database. The results imply effectual outcomes of the JFOFL-MICBCI technique under all runs and samples. For instance, on S1, the JFOFL-MICBCI technique offers *accu$_y$* of 88.62%, 72.68%, 85.73%, 83.67%, and 83.65% underruns 1-5, respectively. Also, on S3, the JFOFL-MICBCI system achieves *accu$_y$* of 89.54%, 81.70%, 95.52%, 76.64%, and 87.52% underruns 1-5, correspondingly. In addition, on S7, the JFOFL-MICBCI technique offers *accu$_y$* of 84.50%, 92.67%, 86.63%, 82.63%, and 96.62% underruns 1-5, respectively. Meanwhile, on S-9, the JFOFL-MICBCI methodology attains *accu$_y$* of 84.50%, 93.76%, 88.52%, 96.60%, and 82.74% underruns 1-5, correspondingly.

Table 4 and Fig. 8 demonstrate an overall comparative study of the JFOFL-MICBCI system on the BCI Competition-IV database. The outcomes exhibited that the CSP model and FBCSP MIRSR systems have attained worse outcomes. At the same time, the FDBN and AORNDL-MIC

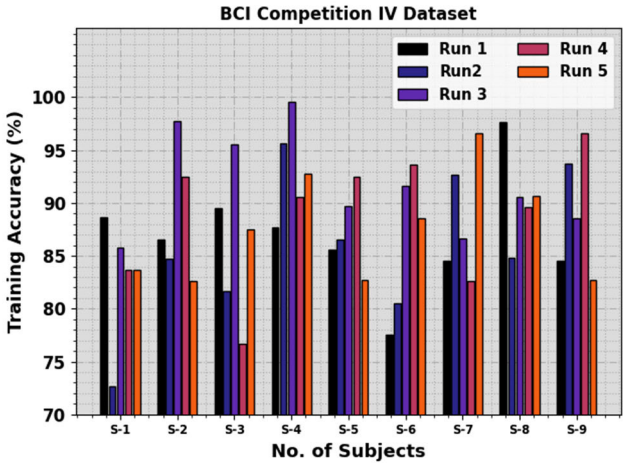

FIGURE 7. Training $accu_y$ outcome of JFOFL-MICBCI technique on BCI Competition-IV database.

TABLE 4. $Accu_y$ outcome of JFOFL-MICBCI technique with other methods on BCI Competition-IV database.

BCI Competition-IV Database					
Subject	CSP	FBCSP MIRSR	FDBN	AORND L-MIC	JFOFL-MICBCI
S-1	67.69	71.54	82.76	82.88	90.61
S-2	63.51	62.65	66.76	88.78	90.36
S-3	58.61	62.78	67.62	86.32	88.00
S-4	98.57	99.50	99.80	93.34	94.89
S-5	78.61	94.67	94.69	87.43	89.17
S-6	76.79	82.58	89.56	86.58	88.38
S-7	78.54	79.62	83.74	88.80	90.50
S-8	94.70	94.63	95.78	90.69	92.45
S-9	84.72	88.75	92.78	89.12	90.82
Average	**77.97**	**81.86**	**85.94**	**88.22**	**90.58**

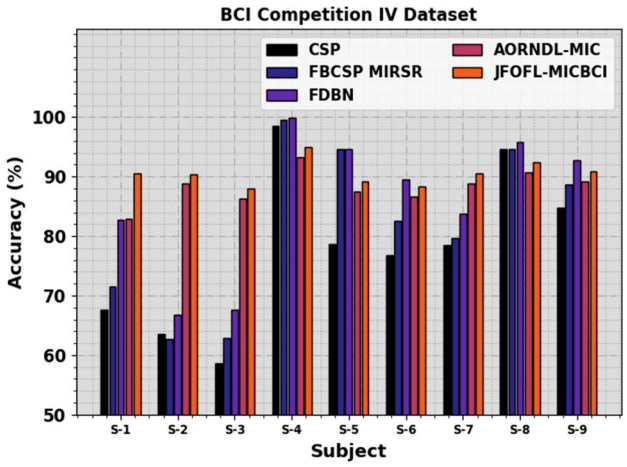

FIGURE 8. $Accu_y$ outcome of JFOFL-MICBCI technique on BCI Competition-IV database.

methods have obtained slightly increased performance. However, JFOFL-MICBCI technology attained maximum performance in all subjects.

Fig. 9 represents an average comparative result of the JFOFL-MICBCI technique on the BCI Competition-IV database. The outcome signified that the JFOFL-MICBCI technique reaches better performance than other models. For instance, the JFOFL-MICBCI technique obtains an increasing average $accu_y$ of 90.58% while the CSP, FBCSP MIRSR, FDBN, and AORNDL-MIC techniques accomplish decreasing average $accu_y$ values of 77.97%, 81.86%, 85.94%, and 88.22% respectively.

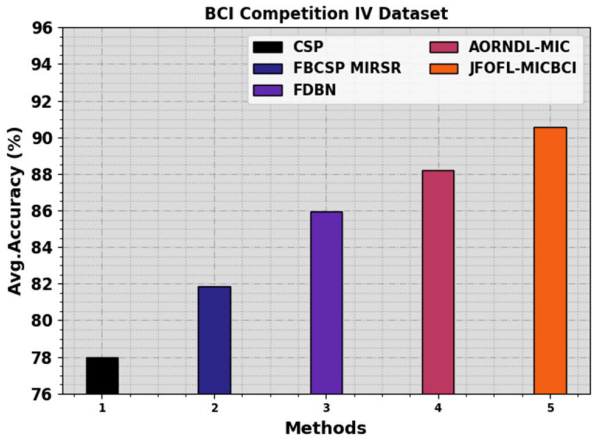

FIGURE 9. Average $Accu_y$ outcome of JFOFL-MICBCI technique on BCI Competition-IV database.

Fig. 10 determines the training accuracy TR_accu_y and VL_accu_y of the JFOFL-MICBCI approach on the BCI Competition-IV database. TL_accu_y determined by the calculation of the JFOFL-MICBCI model on the TR database, while VL_accu_y was computed by estimating the outcome on a separate testing database. The results display that TR_accu_y and VL_accu_y rise with growth in epochs. Thus, the outcome of the JFOFL-MICBCI approach is an increase in the TR and TS database with growth in the amount of epochs.

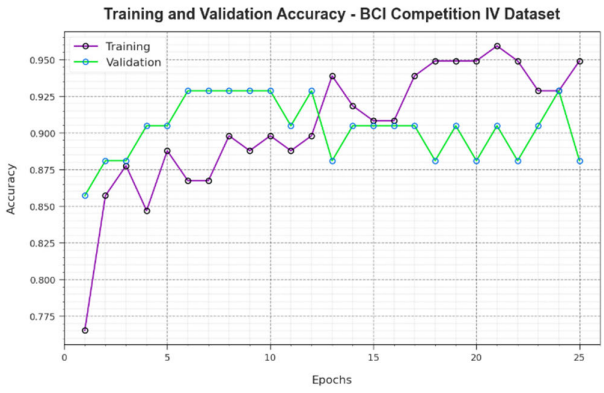

FIGURE 10. $Accu_y$ curve of JFOFL-MICBCI technique on BCI Competition-IV database.

In Fig. 11, *the TR_loss* and *VR_loss* curve of the JFOFL-MICBCI system on the BCI Competition-III database is revealed. The *TR_loss* states an error between the predictive solution and original values on TR data. *VR_loss* signifies a measure of the performance of the JFOFL-MICBCI technique on individual validation data. The results designate that *TR_loss* and *VR_loss* tend to be lesser with

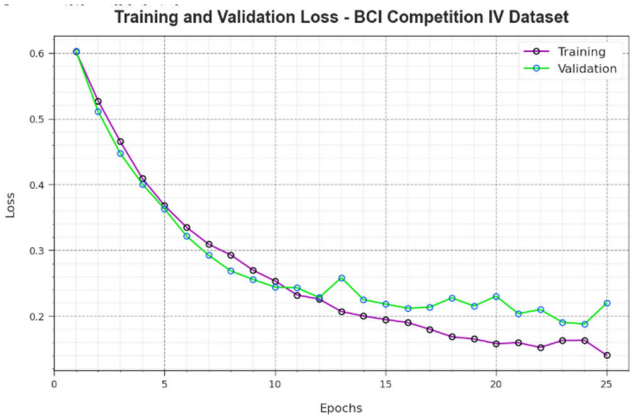

FIGURE 11. Loss curve of JFOFL-MICBCI technique on BCI Competition-IV database.

rising epochs. It described the improved performance of the JFOFL-MICBCI method and its ability to produce an accurate classification. The lesser value of *TR_loss* and *VR_loss* reveals an improved outcome of the JFOFL-MICBCI method on capturing patterns and relationships.

V. CONCLUSION

This manuscript presents an automated EEG Motor Imagery Classification for BCI using the JFOFL-MICBCI method. The main goal of the JFOFL-MICBCI technique is to utilize the FL system with metaheuristics for the classification of EEC motor imagery signals. It comprises different sub-processes such as CWT-based pre-processing, SqueezeNet feature extractor, JFO-based hyperparameter tuning, and ANFIS-based classification. For feature extraction, the JFOFL-MICBCI approach employs the SqueezeNet algorithm, and its hyperparameters can be adjusted by the use of the JFO algorithm. The JFOFL-MICBCI technique has employed the ANFIS model to perform the classification process. A comprehensive range of experiments has been accompanied to demonstrate the high efficiency of the JFOFL-MICBCI algorithm. The obtained outcomes referred to the better of the JFOFL-MICBCI algorithm with other existing systems. In future research, the JFOFL-MICBCI model can be extended to address real-time implementation challenges, aiming for seamless integration into practical BCI applications. Further investigations into optimizing the computational efficiency of the model would be valuable, allowing for faster and more responsive BCI control. Additionally, exploring the adaptability of the JFOFL-MICBCI technique across a broader range of EEG datasets and expanding its capabilities to accommodate more diverse motor imagery tasks could enhance its versatility and applicability in various clinical and assistive technology settings.

REFERENCES

[1] C. Dumitrescu, I.-M. Costea, and A. Semenescu, "Using brain–computer interface to control a virtual drone using non-invasive motor imagery and machine learning," *Appl. Sci.*, vol. 11, no. 24, p. 11876, Dec. 2021, doi: 10.3390/app112411876.

[2] P. Arpaia, A. Esposito, N. Moccaldi, A. Natalizio, and M. Parvis, "Online processing for motor imagery-based brain–computer interfaces relying on EEG," in *Proc. IEEE Int. Instrum. Meas. Technol. Conf. (I2MTC)*, Kuala Lumpur, Malaysia, May 2023, pp. 1–6, doi: 10.1109/I2MTC53148.2023.10176052.

[3] X. Wang, R. Yang, M. Huang, Z. Yang, and Z. Wan, "A hybrid transfer learning approach for motor imagery classification in brain–computer interface," in *Proc. IEEE 3rd Global Conf. Life Sci. Technol. (LifeTech)*, Nara, Japan, Mar. 2021, pp. 496–500, doi: 10.1109/LifeTech52111.2021.9391933.

[4] J. Tong, Z. Xing, X. Wei, C. Yue, E. Dong, S. Du, Z. Sun, J. Solé-Casals, and C. F. Caiafa, "Towards improving motor imagery brain–computer interface using multimodal speech imagery," *J. Med. Biol. Eng.*, vol. 43, no. 3, pp. 216–226, Jun. 2023, doi: 10.1007/s40846-023-00798-9.

[5] D. Li, P. Ortega, X. Wei, and A. Faisal, "Model-agnostic meta-learning for EEG motor imagery decoding in brain–computer-interfacing," in *Proc. 10th Int. IEEE/EMBS Conf. Neural Eng. (NER)*, May 2021, pp. 527–530.

[6] X. Wang, R. Yang, and M. Huang, "An unsupervised deep-transfer-learning-based motor imagery EEG classification scheme for brain–computer interface," *Sensors*, vol. 22, no. 6, p. 2241, Mar. 2022, doi: 10.3390/s22062241.

[7] J. Ma, B. Yang, W. Qiu, Y. Li, S. Gao, and X. Xia, "A large EEG dataset for studying cross-session variability in motor imagery brain–computer interface," *Sci. Data*, vol. 9, no. 1, p. 531, Sep. 2022, doi: 10.1038/s41597-022-01647-1.

[8] A. Singh, A. A. Hussain, S. Lal, and H. W. Guesgen, "A comprehensive review on critical issues and possible solutions of motor imagery based electroencephalography brain–computer interface," *Sensors*, vol. 21, no. 6, p. 2173, Mar. 2021, doi: 10.3390/s21062173.

[9] P. Arpaia, F. Donnarumma, A. Esposito, and M. Parvis, "Channel selection for optimal EEG measurement in motor imagery-based brain–computer interfaces," *Int. J. Neural Syst.*, vol. 31, no. 3, Mar. 2021, Art. no. 2150003, doi: 10.1142/S0129065721500039.

[10] N. Leeuwis, S. Yoon, and M. Alimardani, "Functional connectivity analysis in motor-imagery brain computer interfaces," *Frontiers Hum. Neurosci.*, vol. 15, Oct. 2021, Art. no. 732946, doi: 10.3389/fnhum.2021.732946.

[11] P. Daneshmand, E. Mohammadi, and S. M. S. Khorzooghi, "Electroencephalography-based brain–Computer interface motor imagery classification," *J. Med. Signals Sensors*, vol. 12, no. 1, p. 40, 2022, doi: 10.4103/jmss.JMSS_74_20.

[12] B. Sun, Z. Wu, Y. Hu, and T. Li, "Golden subject is everyone: A subject transfer neural network for motor imagery-based brain computer interfaces," *Neural Netw.*, vol. 151, pp. 111–120, Jul. 2022, doi: 10.1016/j.neunet.2022.03.025.

[13] T. Khanam, S. Siuly, and H. Wang, "An optimized artificial intelligence based technique for identifying motor imagery from EEGs for advanced brain computer interface technology," *Neural Comput. Appl.*, vol. 35, no. 9, pp. 6623–6634, Mar. 2023, doi: 10.1007/s00521-022-08027-1.

[14] D. Jaipriya and K. C. Sriharipriya, "Brain computer interface-based signal processing techniques for feature extraction and classification of motor imagery using EEG: A literature review," *Biomed. Mater. Devices*, vol. 2023, pp. 1–12, May 2023, doi: 10.1007/s44174-023-00082-z.

[15] A. Nandhini and J. Sangeetha, "A review on deep learning approaches for motor imagery EEG signal classification for brain–computer interface systems," in *Proc. ICCVBIC*, 2023, pp. 353–365, doi: 10.1007/978-981-19-9819-5_27.

[16] M. T. Sadiq, X. Yu, Z. Yuan, M. Z. Aziz, S. Siuly, and W. Ding, "Toward the development of versatile brain–computer interfaces," *IEEE Trans. Artif. Intell.*, vol. 2, no. 4, pp. 314–328, Aug. 2021, doi: 10.1109/TAI.2021.3097307.

[17] X. Yu, M. Z. Aziz, M. T. Sadiq, Z. Fan, and G. Xiao, "A new framework for automatic detection of motor and mental imagery EEG signals for robust BCI systems," *IEEE Trans. Instrum. Meas.*, vol. 70, pp. 1–12, 2021, doi: 10.1109/TIM.2021.3069026.

[18] H. Akbari, M. T. Sadiq, M. Payan, S. S. Esmaili, H. Baghri, and H. Bagheri, "Depression detection based on geometrical features extracted from SODP shape of EEG signals and binary PSO," *Traitement Signal*, vol. 38, no. 1, pp. 13–26, Feb. 2021, doi: 10.18280/ts.380102.

[19] H. Akbari, M. T. Sadiq, N. Jafari, J. Too, N. Mikaeilvand, A. Cicone, and S. Serra-Capizzano, "Recognizing seizure using Poincaré plot of EEG signals and graphical features in DWT domain," *Bratislava Med. J.*, vol. 124, no. 1, pp. 12–24, 2022, doi: 10.4149/BLL_2023_002.

[20] M. T. Sadiq, H. Akbari, S. Siuly, Y. Li, and P. Wen, "Alcoholic EEG signals recognition based on phase space dynamic and geometrical features," *Chaos, Solitons Fractals*, vol. 158, May 2022, Art. no. 112036, doi: 10.1016/j.chaos.2022.112036.
[21] R. Sharma, M. Kim, and A. Gupta, "Motor imagery classification in brain-machine interface with machine learning algorithms: Classical approach to multi-layer perceptron model," *Biomed. Signal Process. Control*, vol. 71, Jan. 2022, Art. no. 103101, doi: 10.1016/j.bspc.2021.103101.
[22] A. Subasi and S. Mian Qaisar, "The ensemble machine learning-based classification of motor imagery tasks in brain–computer interface," *J. Healthcare Eng.*, vol. 2021, pp. 1–12, Nov. 2021, doi: 10.1155/2021/1970769.
[23] G. Liu, J. H. Hsiao, W. Zhou, and L. Tian, "MartMi-BCI: A MATLAB-based real-time motor imagery brain–computer interface platform," *SoftwareX*, vol. 22, May 2023, Art. no. 101371, doi: 10.1016/j.softx.2023.101371.
[24] F. Mattioli, C. Porcaro, and G. Baldassarre, "A 1D CNN for high accuracy classification and transfer learning in motor imagery EEG-based brain–computer interface," *J. Neural Eng.*, vol. 18, no. 6, Dec. 2021, Art. no. 066053, doi: 10.1088/1741-2552/ac4430.
[25] S. Mirzaei and P. Ghasemi, "EEG motor imagery classification using dynamic connectivity patterns and convolutional autoencoder," *Biomed. Signal Process. Control*, vol. 68, Jul. 2021, Art. no. 102584, doi: 10.1016/j.bspc.2021.102584.
[26] A. Abdul Ameer Abbas and H. Martínez-García, "Real-time motor imagery-based brain–computer interface system by implementing a frequency band selection," *Arabian J. Sci. Eng.*, vol. 48, no. 11, pp. 15099–15113, Nov. 2023, doi: 10.1007/s13369-023-08024-z.
[27] A. Kamble, P. Ghare, and V. Kumar, "Machine-learning-enabled adaptive signal decomposition for a brain–computer interface using EEG," *Biomed. Signal Process. Control*, vol. 74, Apr. 2022, Art. no. 103526, doi: 10.1016/j.bspc.2022.103526.
[28] R. Dhiman, "Electroencephalogram channel selection based on Pearson correlation coefficient for motor imagery-brain–computer interface," *Meas., Sensors*, vol. 25, Feb. 2023, Art. no. 100616, doi: 10.1016/j.measen.2022.100616.
[29] M. T. Sadiq, X. Yu, Z. Yuan, F. Zeming, A. U. Rehman, I. Ullah, G. Li, and G. Xiao, "Motor imagery EEG signals decoding by multivariate empirical wavelet transform-based framework for robust brain–computer interfaces," *IEEE Access*, vol. 7, pp. 171431–171451, 2019, doi: 10.1109/ACCESS.2019.2956018.
[30] M. T. Sadiq, X. Yu, Z. Yuan, and M. Z. Aziz, "Motor imagery BCI classification based on novel two-dimensional modelling in empirical wavelet transform," *Electron. Lett.*, vol. 56, no. 25, pp. 1367–1369, Dec. 2020, doi: 10.1049/el.2020.2509.
[31] M. T. Sadiq, X. Yu, Z. Yuan, M. Z. Aziz, N. U. Rehman, W. Ding, and G. Xiao, "Motor imagery BCI classification based on multivariate variational mode decomposition," *IEEE Trans. Emerg. Topics Comput. Intell.*, vol. 6, no. 5, pp. 1177–1189, Oct. 2022, doi: 10.1109/TETCI.2022.3147030.
[32] X. Geng, D. Li, H. Chen, P. Yu, H. Yan, and M. Yue, "An improved feature extraction algorithms of EEG signals based on motor imagery brain–computer interface," *Alexandria Eng. J.*, vol. 61, no. 6, pp. 4807–4820, Jun. 2022, doi: 10.1016/j.aej.2021.10.034.
[33] B. Sun, Z. Liu, Z. Wu, C. Mu, and T. Li, "Graph convolution neural network based end-to-end channel selection and classification for motor imagery brain–computer interfaces," *IEEE Trans. Ind. Informat.*, vol. 19, no. 9, pp. 9314–9324, Sep. 2023, doi: 10.1109/TII.2022.3227736.
[34] A. Tiwari, "A logistic binary Jaya optimization-based channel selection scheme for motor-imagery classification in brain–computer interface," *Expert Syst. Appl.*, vol. 223, Aug. 2023, Art. no. 119921, doi: 10.1016/j.eswa.2023.119921.
[35] N. Yahya, H. Musa, Z. Y. Ong, and I. Elamvazuthi, "Classification of motor functions from electroencephalogram (EEG) signals based on an integrated method comprised of common spatial pattern and wavelet transform framework," *Sensors*, vol. 19, no. 22, p. 4878, Nov. 2019, doi: 10.3390/s19224878.
[36] H. Lee, I. Ullah, W. Wan, Y. Gao, and Z. Fang, "Real-time vehicle make and model recognition with the residual SqueezeNet architecture," *Sensors*, vol. 19, no. 5, p. 982, Feb. 2019, doi: 10.3390/s19050982.
[37] D. Yadav, N. Singh, V. S. Bhadoria, N. C. Giri, and M. Cherukuri, "A novel metaheuristic jellyfish optimization algorithm for parameter extraction of solar module," *Int. Trans. Electr. Energy Syst.*, vol. 2023, pp. 1–21, Jul. 2023, doi: 10.1155/2023/5589859.
[38] C. Iwendi, K. Mahboob, Z. Khalid, A. R. Javed, M. Rizwan, and U. Ghosh, "Classification of COVID-19 individuals using adaptive neuro-fuzzy inference system," *Multimedia Syst.*, vol. 28, no. 4, pp. 1223–1237, Aug. 2022, doi: 10.1007/s00530-021-00774-w.
[39] S. Lemm, C. Schafer, and G. Curio, "BCI competition 2003-data set III: Probabilistic modeling of sensorimotor μ-rhythms for classification of imaginary hand movements," *IEEE Trans. Biomed. Eng.*, vol. 51, no. 6, pp. 1077–1080, Jun. 2004, doi: 10.1109/TBME.2004.827076.
[40] R. Leeb, F. Lee, C. Keinrath, R. Scherer, H. Bischof, and G. Pfurtscheller, "Brain–computer communication: Motivation, aim, and impact of exploring a virtual apartment," *IEEE Trans. Neural Syst. Rehabil. Eng.*, vol. 15, no. 4, pp. 473–482, Dec. 2007, doi: 10.1109/TNSRE.2007.906956.
[41] A. A. Malibari, F. N. Al-Wesabi, M. Obayya, M. A. Alkhonaini, M. A. Hamza, A. Motwakel, I. Yaseen, and A. S. Zamani, "Arithmetic optimization with RetinaNet model for motor imagery classification on brain computer interface," *J. Healthcare Eng.*, vol. 2022, pp. 1–11, Mar. 2022, doi: 10.1155/2022/3987494.

EUNMOK YANG received the M.S. degree from the Department of Computer Engineering, Kongju National University, Gongju, South Korea, in 2002, and the Ph.D. degree from the Department of Mathematics, Kongju National University, in 2016. In 2016, he was with the UbiTech Research Center. Since 2017, he has been a Researcher with Soongsil University's Industry–University Cooperation Foundation. Since 2020, he has been a Research Professor with the Kookmin University's Department of Financial Information Security. His research interests include security, artificial intelligence, data mining, machine learning, and network security.

K. SHANKAR (Senior Member, IEEE) received the Ph.D. degree in computer science from Alagappa University, Karaikudi, India. He is currently a Postdoctoral Fellow with the Big Data and Machine Learning Laboratory, South Ural State University, Russia; and an Adjunct Faculty of the Department of Computer Science and Engineering, Saveetha School of Engineering, Saveetha Institute of Medical and Technical Sciences, Chennai, India. He has authored/coauthored more than 150 ISI journal articles (with total Impact Factor more than 350) and more than 100 Scopus-indexed articles. He has also authored/edited six international books published by recognized publishers, such as Springer and CRC. His research interests include healthcare applications, secret image sharing scheme, digital image security, cryptography, the Internet of Things, and optimization algorithms.

ESWARAN PERUMAL received the M.Sc. degree in computer science and information technology from Madurai Kamaraj University, India, in 2003, and the M.Tech. and Ph.D. degrees in computer and information technology from Manonmaniam Sundaranar University, India, in 2005 and 2010 respectively.

In 2010, he joined the Department of Computer Science and Engineering, PSN College of Engineering and Technology, as an Assistant Professor. Since May 2012, he has been with the Department of Computer Applications, Alagappa University, Karaikudi, India. He has published more than 75 research articles in reputed SCI/Scopus indexed journals and presented his research findings in IEEE international conferences. He has written book chapters in the area of blockchain technology, cryptography, Robots in the Disease Recovery Process in springer and Taylor & Francis. He has authored a book in the title of ''Artificial Intelligence for the Internet of Health Things'' published by Taylor & Francis (CRC Press). He has supervised eight PhD, 27 M.Phil., and more than 70 master's students. His area of research interests includes digital image processing, focusing on color image edge detection, artificial intelligence, big data analytics, data science, and data visualization.

Dr. Perumal has a member of the review board for many international journals, conferences, and committees. He was the recipient of JRF & SRF Award of the University Grants Commission, Govt. of India, New Delhi in the year 2008 for his doctoral study (Ph.D.). He was awarded Vallal Alagappar Research Recognition Award-2020 and Promising Researcher Award-2022 by Alagappa University, Karaikudi, India

CHANGHO SEO received the B.S., M.S., and Ph.D. degrees in mathematics from Korea University, Seoul, South Korea, in 1990, 1992, and 1996, respectively. He is currently a Full Professor with the Department of Convergence Science, Kongju National University, South Korea. His research interests include cryptography, information security, data privacy, and system security.